ARTICLE

Infantile Encephalopathy and Defective Mitochondrial DNA Translation in Patients with Mutations of Mitochondrial Elongation Factors EFG1 and EFTu

Lucia Valente, Valeria Tiranti, René Massimiliano Marsano, Edoardo Malfatti, Erika Fernandez-Vizarra, Claudia Donnini, Paolo Mereghetti, Luca De Gioia, Alberto Burlina, Claudio Castellan, Giacomo P. Comi, Salvatore Savasta, Iliana Ferrero, and Massimo Zeviani

Mitochondrial protein translation is a complex process performed within mitochondria by an apparatus composed of mitochondrial DNA (mtDNA)–encoded RNAs and nuclear DNA–encoded proteins. Although the latter by far outnumber the former, the vast majority of mitochondrial translation defects in humans have been associated with mutations in RNA-encoding mtDNA genes, whereas mutations in protein-encoding nuclear genes have been identified in a handful of cases. Genetic investigation involving patients with defective mitochondrial translation led us to the discovery of novel mutations in the mitochondrial elongation factor G1 (EFG1) in one affected baby and, for the first time, in the mitochondrial elongation factor Tu (EFTu) in another one. Both patients were affected by severe lactic acidosis and rapidly progressive, fatal encephalopathy. The EFG1-mutant patient had early-onset Leigh syndrome, whereas the EFTu-mutant patient had severe infantile macrocystic leukodystrophy with micropolygyria. Structural modeling enabled us to make predictions about the effects of the mutations at the molecular level. Yeast and mammalian cell systems proved the pathogenic role of the mutant alleles by functional complementation in vivo. Nuclear-gene abnormalities causing mitochondrial translation defects represent a new, potentially broad field of mitochondrial medicine. Investigation of these defects is important to expand the molecular characterization of mitochondrial disorders and also may contribute to the elucidation of the complex control mechanisms, which regulate this fundamental pathway of mtDNA homeostasis.

The mitochondrial respiratory chain (MRC) is a multiheteromeric enzymatic structure that performs oxidative phosphorylation (OXPHOS), a fundamental reaction of life that supplies ~90% of the energy used by mammalian cells.[1] The MRC consists of five complexes, composed of ~85 structural proteins, 13 of which are encoded by mtDNA, whereas the others are encoded by nuclear genes. The 13 mtDNA-encoded polypeptides (designated "*mit*" genes, according to the yeast mtDNA terminology) are integral parts of four MRC complexes; seven are subunits of complex I (cI), one is a subunit of complex III (cIII), three are subunits of complex IV (cIV, or cytochrome c oxidase [COX]), and two are subunits of complex V (cV). Complex II (cII, or succinate:ubiquinone oxidoreductase) is the only MRC complex that lacks mtDNA-encoded subunits. The *mit* genes are translated into proteins within the organelles by a protein-synthesis machinery, composed of both RNAs and proteins, which is largely independent from that responsible for translation of genes contained in the nuclear genome, which takes place in the cytosol. The RNA component of mitochondrial translation consists of 22 tRNAs and 2 ribosomal RNAs (rRNAs) encoded by mtDNA genes (designated "*syn*" genes, according to the yeast terminology), whereas the protein component is encoded by nuclear genes and consists of ~50 ribosomal proteins; several tRNA maturation enzymes; the aminoacyl-tRNA synthetases; the translation initiation, elongation, and termination factors; and likely a large number of unidentified factors, including ribosome-assembly factors.[2,3] Abnormalities in either gene set—mitochondrial or nuclear—can compromise mitochondrial translation; as a consequence, multiple biochemical defects may occur in the mtDNA-dependent MRC complexes, leading to faulty OXPHOS and disease. Over 100 disease-causing mutations are known in either tRNA- or rRNA-encoding mtDNA *syn* genes (Mitomap). In contrast, only a few patients have been reported with mutations in mitochondrial translation protein factors. More precisely, a missense mutation in pseudouridine synthase 1 (PUS1) was identified in Persian Jewish families affected by myopathy, lactic acidosis, and sideroblastic anemia (MLASA [MIM #600462]). PUS1 converts uridine into pseudouridine in several positions of tRNAs synthesized in both nuclear and mitochondrial compartments[4,5]; lack

From the Pierfranco and Luisa Mariani Center for Research on Children's Mitochondrial Disorders, Division of Molecular Neurogenetics, Institute of Neurology "Carlo Besta"–IRCCS Foundation (L.V.; V.T.; E.M.; E.F.-V.; M.Z.), Department of Biotechnology and Biosciences, University of Milano-Bicocca (P.M.; L.D.G.), and Dino Ferrari Center, Department of Neurological Sciences, University of Milan, IRCCS Foundation Ospedale Maggiore Policlinico, Mangiagalli and Regina Elena (G.P.C.), Milan, Italy; Department of Genetics, Biology of Microrganisms, Anthropology, and Evolution, University of Parma, Parma, Italy (R.M.M.; C.D.; I.F.); Department of Neurology, University of Siena, Siena, Italy (E.M.); Department of Paediatrics, University of Padua, Padua, Italy (A.B.); Service of Genetics, Regional Public Health Hospital, Bolzano, Italy (C.C.); and Department of Paediatrics, University of Pavia, Pavia, Italy (S.S.)

Received August 1, 2006; accepted for publication October 25, 2006; electronically published November 15, 2006.

Address for correspondence and reprints: Dr. Massimo Zeviani, Division of Molecular Neurogenetics, National Neurological Institute "Carlo Besta," via Temolo 4, Milano 20126, Italy. E-mail: zeviani@istituto-besta.it

Am. J. Hum. Genet. 2007;80:44–58. 0002-9297/2007/8001-0006$15.00

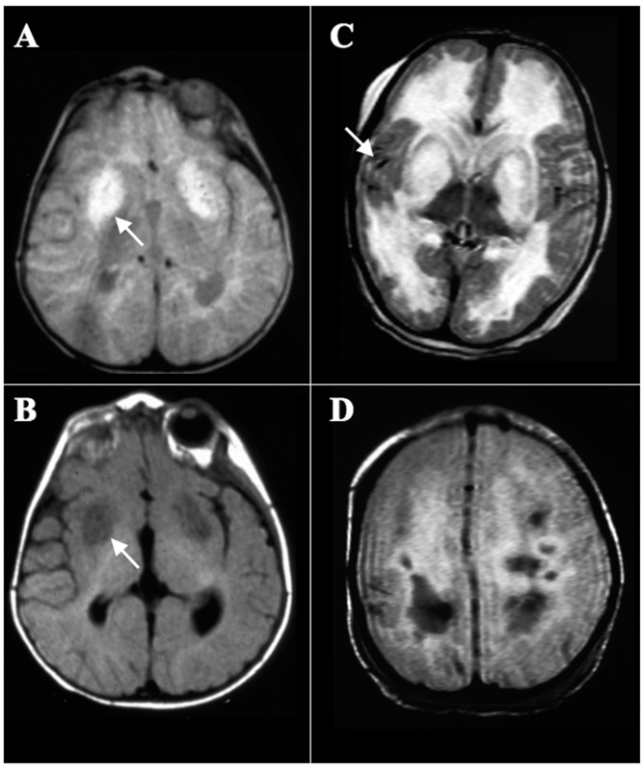

Figure 1. Brain MRIs of patient I.V. (*A* and *B*) and patient S.S. (*C* and *D*). *A,* T2-weighted coronal section showing hyperintense symmetric lesions of the putamen and globus pallidus (*arrow*). *B,* T1-weighted image of the same section as in panel A, showing hypointense abnormal signals (*arrow*) corresponding to those shown in A. *C,* T2-weighted coronal section showing diffuse hyperintensity of the centra semiovalia and basal ganglia. The arrow indicates an area of micropolygyria in the right perisylvian region. *D,* T2-weighted coronal section showing diffuse hyperintensity and multiple cysts of the white matter.

of this posttranscriptional maturation of tRNAs leads to defective cytosolic and mitochondrial translation. A second observation concerned a homozygous stop mutation in MRPS16 (MIM *609204), a protein of the mitochondrial small ribosomal subunit, which was found in one infant with severe lactic acidosis, developmental defects in the brain, and facial dysmorphisms.[6] A missense mutation in the mitochondrial elongation factor G1 (EFG1) was found in a singleton case affected by fatal neonatal liver failure and lactic acidosis associated with severe mitochondrial translation defect (combined oxidative phosphorylation deficiency 1 [MIM #609060]).[7] Combined nonsense and missense mutations in the same gene were later found in two compound heterozygous brothers with a similar syndrome.[8] Finally, the same homozygous missense mutation in the mitochondrial translation elongation factor Ts (EFTs) has recently been reported in two unrelated babies, one affected by mitochondrial encephalomyopathy, the other by fatal hypertrophic cardiomyopathy.[9] However, since nearly 200 nuclear-encoded proteins participate in the translation of mitochondrial transcripts, it is reasonable to assume that defects in these proteins are either lethal or are underdiagnosed to a major extent.

We report here the results of a study involving two unrelated infants affected by neonatal lactic acidosis, rapidly progressive encephalopathy, severely decreased mitochondrial protein synthesis, and combined deficiency of mtDNA-related MRC complexes. One patient carried two novel allelic mutations in the elongation factor EFG1; the other is the first patient harboring a homozygous mutation in the elongation factor Tu (EFTu).

Case Reports

Patient I.V.

Patient I.V. was the second daughter of Italian, nonconsanguineous, unaffected parents. The patient was born at term after an uneventful pregnancy. The mother had previously had a spontaneous early miscarriage. Family history was negative for neurological disease. The patient's 14-year-old sister is alive and well.

At birth, the baby had the following measurements: weight 3,300 g, body length 49 cm, head circumference 35 cm. At age 7 d, she was evaluated for the presence of dysmorphic signs, including flat nasal bridge, low-set ears, small hands and feet, epicanthus, and high, arched palate. A total-body radiograph showed short tibial bones, whereas the results of brain and kidney ultrasound, thyroid hormone levels, electrocardiogram (ECG), and fundus oculi were normal. At age 3 wk, the patient started having feeding difficulties and gain loss. The karyotype was 46,XX, with no chromosomal abnormalities.

At age 3 mo, the neurological examination showed reduced spontaneous movements and severe axial hypotonia, with preservation of deep tendon reflexes. Blood creatine kinase, transaminases, lactate dehydrogenase, and ammonia levels were normal. The ECG remained normal, but an electroencephalogram showed global, severe disorganization with complete lack of sleep spindles.

At age 5 mo, she presented with recurrent episodes of vomiting. Plasma and urinary amino acids were normal, as were plasma carnitine, mucopolysaccharides, and long-chain fatty acids. Urine organic-acids analysis showed increased lactic and β-hydroxybutyrate. Blood lactic acid was 5.2 mM (normal values [nv] <2.2), blood pyruvate was 0.46 mM (nv < 0.2), and blood β-hydroxybutyrate was 0.39 mM (nv < 0.1). The combined increase of both lactate and pyruvate suggests the presence of a very severe retrograde block of glucose utilization in this patient.

Brain magnetic resonance imaging (MRI) showed two large, bilateral and symmetrical areas of increased T2 (fig. 1*A*) and decreased T1 signals (fig. 1*B*) involving the putamen and the globus pallidus. Similar signal changes were detected in the rostral mesencephalon, and there was delayed frontal myelination.

The patient was given treatment with ubidecarenone, riboflavin, and thiamine; feeding problems were addressed

Table 1. PCR Primers and Annealing Temperatures Specific to Human *EFG1* and *EFTu* Genes

Gene and Exons	Primer Sequence (5′→3′) Forward	Reverse	Annealing Temperature (°C)
EFG1[a]:			
1	CCTCACTCTCTTTTTCCTCGC	CCCAGAAGGGATCACAAGGT	54
2	GGTGCCTTTCTCAAGCTATCT	TCAAAAGTCCGCTGTTACCATTG	55
3	TCTTGGAATGCAGGGACAGAG	GCTCTAGGTCCTAAGTTAGTCT	54
4	GACTTATGTGATGAGCAGAGATA	GGATATAAGGTTTGCTGTCTAGA	54
5	CAAAGGGATTAGGGGAGAAGA	AGATAGTTACTCTGCGTTTGATGA	55
6	ATGTATCAGAGCTCTTTGTTACC	ATAAAAGCATCATGTCCCCTCCC	56
7	GTTGACTTGAAGCACAACATG	TCCTTAAATTCCTTCACAGTGCA	53
8	ACTTATTGTGTGACAGCAGTAATATCC	GAACTATCATGTCAGAGCTTTGGA	55
9	CTTGGAGGGAGTTATGAAGCT	CTATTTCACCCACATCAGAGGAAT	55
10	CAATGTGTGTACTGTACAGTTTAC	CTCAACGAAAACTTCTGTGGTTGT	55
11	GTCTAGCCTAAAGACATAGGC	ACCAACAGAGGAAATAGAGACC	55
12	TCCCATTGCTTATCATGCTCAG	GTGACGCATGAAGAACCAGAG	56
13	GCTTAGGAGGTTTTCTTTCGG	CAGTAATAGTGGTATGTATATCCA	55
14	TTACCTTGGGTAGTATACCCCA	GTGATAGACAACATGATGGAAG	55
15	GGGGTTCTTGATAATGTATCTGC	TGAGGCTATGATGATCTATCAGG	54
16	GTGTTTGTACCTTTGGAAAGCAT	TCAGCAAGGAAATGTGTCCATTTG	56
17/18	AGGCTGTCAATGGTGTTCACT	CGCAGATTCAATTAGAGTCAGTC	55
EFTu[b]:			
1/2	AGCTCTAACTTCCGCCGGAA	TCCAGGTCCCATCAGTAGATA	55
3	TGCCTCTAGCACTGGAACTT	TCCTGACAAGAGGCAGCTTCT	55
4/5	GTGAACTGAAGAGCTCGTTG	AGACACAAAGCAGAGCTCTG	55
6/7	CAGAGCTCTGCTTTGTGTCT	AGAGGGAAGGCACAAGGGA	55
8/9	TCCCTTGTGCCTTCCCTCT	GGAACTATGAGTGAAGCAAAGG	56
10	TTAAGGAATGAAGGCACCCTGG	TCCTCCCCTATCCTCTCCAAT	56

[a] NCBI accession number NM_024996.
[b] NCBI accession number NM_003321.

with nasogastric feeding. Nevertheless, her weight at age 14 mo was 7,530 g, well below the 3rd percentile. The hepatic enzymes, bilirubin, and ammonia remained consistently normal in the blood during the entire course of her life, and no sign of liver involvement was ever detected. However, she had microcephalia, severely delayed motor and mental development, decreased axial and increased limb muscle tone, brisk deep-tendon reflexes, and purposeless movements. Lactic acid was persistently high. At age 16 mo, the patient died from a respiratory insufficiency. The family declined to have an autopsy performed.

Patient S.S.

Patient S.S. was the second daughter of reportedly nonconsanguineous, unaffected parents, originating from a small village in an isolated valley of Italian South Tyrol. She was born at term after an uneventful pregnancy. Family history was negative for neurological disease. Her 20-year-old brother is alive and well. The karyotype was 46,XX, with no abnormalities.

At birth, the baby had the following measurements: weight 2,770 g, body length 48 cm, and head circumference 31 cm. At 2 d after birth, she developed acute respiratory distress and severe metabolic acidosis (pH 7.2; PCO_2 15 mmHg; PO_2 60 mmHg; O_2 saturation 90%; base excess −26 mM), with two episodes of generalized hypertonus and opisthotonus. Serum lactic acid was 10.2 mM (nv < 2.2 mM). A brain CT scan showed several hypodense lesions in the right parietal and bilateral periventricular regions. The patient had occasionally high serum ammonia (143 mg/dl; nv < 75 mg/dl) and mildly elevated serum transaminases (serum glutamic oxaloacetic transaminase 106 U/liter; nv < 42 U/liter; serum glutamic pyruvic transaminase 51 U/liter; nv < 38 U/liter). ECG showed signs of myocardial ischemia. The lactic acidosis was partially corrected by intravenously administered bicarbonate. She was relatively well until age 6 mo, when she had another episode of severe metabolic crisis, characterized by persistent vomiting, lethargy, skin pallor, and acral cyanosis, because of acute metabolic acidosis (pH 7.04; PCO_2 24.1 mmHg; PO_2 46.7 mmHg; base excess −24.2 mM). Serum lactate was 86 mM, ammonia was 89 mg/dl. In the following weeks, several episodes of acute metabolic acidosis were corrected by intravenous administration of bicarbonate. The acute episodes punctuated a relentless downhill course characterized by severe psychomotor regression with microcephaly, generalized axial hypotonia with limb spasticity, and nystagmus. The liver was enlarged. Brain MRI at age 8 mo showed the presence of micropolygyria in the right perisylvian region and diffuse signal abnormality of the white matter in the centra semiovalia, putamina, and nuclei pallidi (fig. 1*C*), with multiple cystic lesions (fig. 1*D*); marked alterations of the

white matter were also present in the brain stem and, although to a lesser extent, in the cerebellum (not shown).

The patient died at age 14 mo. The family declined to have an autopsy performed.

Material and Methods

Patients and DNA Samples

We obtained institutional review board–approved informed consent from parents of all probands and siblings before collecting blood for DNA extraction or performing tissue biopsies.

Sequence Analysis

Nucleotide sequence analysis was performed on a 3100 ABI Automated Sequencer on samples prepared using the BigDye Termination kit (Applied Biosystems). Data were elaborated using the Secscape software (Applied Biosystems). The oligonucleotide primers used for PCR amplification of the 18 exons of the human *EFG1* (NCBI accession number NM_024996) and the 10 exons of the human EFTu encoding *TUFM* (NCBI accession number NM_003321) genes are listed in table 1. PCR amplification conditions were as follows: an initial denaturation step at 95°C for 1 min; 30 cycles of denaturation at 95°C for 1 min, annealing at different temperatures (depending on the primers used; table 1) for 30 s, and extension at 72°C for 1 min; and a final extension at 72°C for 5 min.

Generation and Cloning of Human Mitochondrial EFG1 and EFTu

The full-length human IMAGE cDNA clones for *Homo sapiens EFG1* and *EFTu* were obtained from the RZPD German Resource Center (*EFG1* clone IRATp970B0374D; *EFTu* clone IRAUp969C0361D). The two cDNA inserts were amplified using the following primers: for EFG1, forward primer 5′-CACCCGTTACCGGCAGCTGAACC-3′ and reverse primer 5′-CAAAACCACGCAGATTCAATTAGAGTC-3′ and, for EFTu, forward primer 5′-CACCCTGTGCGCTCGGGCTCCTGG-3′ and reverse primer 5′-AGCCCTGGCTAGGGCAGGCCTTAAAC-3′ (the underlined sequence at 5′ end of the forward primers is added to provide a sticky ends necessary for directional cloning). The PCR products were then cloned into the pcDNA3.2/V5/GW/D-TOPO vector (Invitrogen). The recombinant plasmids were transfected by electroporation in patients' fibroblasts, as described elsewhere,[10] and were selected with 200 μg/ml of the neomycin analogue drug G418. For retrotranscription of EFTu RNA, the AMV kit cDNA (Invitrogen) was used in accordance with the manufacturer's protocol.

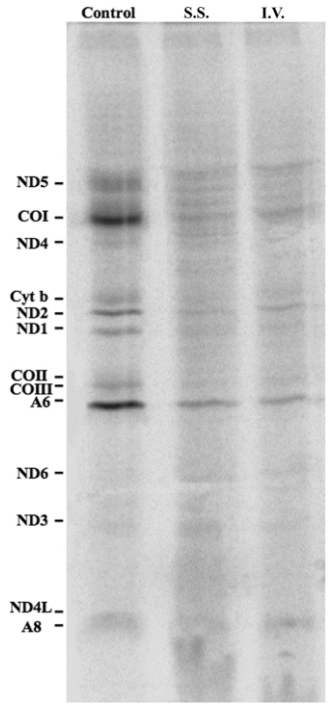

Figure 2. mtDNA-specific protein synthesis on fibroblasts from a control, patient S.S., and patient I.V. The autoradiographic bands are labeled according to standard nomenclature: ND1, ND2, ND3, ND4, ND4L, ND5, and ND6 are subunits of cI; Cyt b is cytochrome b, a subunit of cIII; COI, COII, and COIII are subunits of cIV; and A6 and A8 are subunits of cV.

Mammalian Cell Cultures

Mammalian cells were cultured in Dulbecco's modified Eagle medium (DMEM) (4.5 g/liter glucose), supplemented with 0.1 mM of Na pyruvate, 50 μg/ml uridine, 200 U/ml penicillin/streptomycin, 2 mM glutamine, and 10% fetal calf serum, at 37°C in a 5%-CO_2 atmosphere. Selection in galactose was performed using medium containing DMEM (without glucose), 25 mM galactose, 10% dyalized calf serum, 200 U/ml penicillin/streptomycin, and 2 mM glutamine.

Patients' fibroblasts were transfected, with plasmid pBABE carrying resistance to puromycin,[11] whereas 143B ρ° cells were transfected with plasmid pRNS-1 carrying resistance to G418.[11] Patients' fibroblasts and 143B ρ° cells were cocultured overnight, were fused with a solution of poly-ethylene glycol in phosphate buffer, and were selected, after 24 h, in a medium containing 200 μg/ml of G418 and 0.5 μg/ml of puromycin.[11]

Biochemical assays were performed after 2 wk of selection,

Table 2. Yeast Strains

Strain	Genotype	Source
BY4741Δ*mef1*	MAT**a**; *his3*Δ1 *leu2*Δ0 *lys2*Δ0 *ura3*Δ0; *YLR069c::kanMX4*	Euroscarf collection
BY4741Δ*tuf1mef1*BY4741Δ*mef1*	MAT**a**; *his3*Δ1 *leu2*Δ0 *lys2*Δ0 *ura3*Δ0; *YOR187w::kanMX4*	Euroscarf collection
W303-1B	MATα *ade2 his3 leu2 trp1 ura3*	R. Rothstein collection
TUW	Cross of BY4741 Δ*tuf1* and W303-1B	Present study
MEW	Cross of BY4741 Δ*mef1* and W303-1B	Present study
EB-4B	MATα *ade2 his3 leu2 trp1 ura3 MIP1::kanMX4 sml1::HIS3* ρ0	I. Ferrero collection

Table 3. Oligonucleotides Used for Site-Directed Mutagenesis and for Cloning and Sequencing

Oligonucleotide Use and Name	Sequence (5′→3′)	Amino Acid Change
Site-directed mutagenesis[a]:		
MEF1for	AAAGAAACAATTATTTCTGGGAGAGGTGAATTGCATCTGGAGATT	M516R
MEF1rev	AATCTCCAGATGCAATTCACCTCTCCCAGAAATAATTGTTTCTTT	
TUF1for	TCAGGAGAGATCAATTGAAGCAAGGTATGGTCTTAGCTAAGCCA	R325Q
TUF1rev	TGGCTTAGCTAAGACCATACCTTGCTTCAATTGATCTCTCCTGAT	
Cloning and sequencing[b]:		
MEF1for	*ATCGGAATTC*TTGAGGGCCCGGAATGAAG	
MEF1rev	*ATCGGCATGC*TATGCCGTACCAGAAAAGGAAC	
MEF1seq1	GTCTGCCGCTACTTACTGCTCT	
MEF1seq2	CCTAATCCCTCTGAAGTGTTGAAT	
MEF1seq3	AGAATCCACGGCATGAATAGCAC	
TUF1for	*AGGATCC*CTTCATCGCCTGCTTACTACTTTG	
TUF1rev	*AGCATGC*ACGCCTTTAACTTTCTCCCGACTA	
TUF1seq1	TTTAGCACCCATCCGACCTCAGT	
TUF1seq2	GTTAGCCGCAAAAGGTGGTG	
TUF1seq3	CTGGTCGTGTGGAAAGGGGTAAT	

[a] Base changes are underlined.
[b] Sequences in italic at the 5′ end of the primer have been added to provide the ends necessary for cloning.

when both parental cells and homodicaryon hybrids, grown in the selection medium, were completely eliminated. Characterization of the nuclear DNA in the resulting heterodikaryons was performed using a highly polymorphic repetitive sequence at the *D11S533* locus, as described elsewhere.[12]

Western-Blot Analysis

Mitochondria were isolated from cultured fibroblasts as described elsewhere.[13] Analysis by SDS-polyacrylamide gel of 100 μg protein/lane and western-blot analysis were performed as described elsewhere,[14] by use of the ECL-chemiluminescence kit (Amersham).

Antibodies

An affinity purified polyclonal anti-mammalian EFTu+EFTs antibody[15] was a kind gift of Professor Linda Spremulli (University of North Carolina at Chapel Hill). A mouse monoclonal antibody against the 70-kDa subunit of mammalian succinate dehydrogenase was from Molecular Probes–Invitrogen.

Table 4. MRC Activities of cI–cV on Homogenate, Normalized to the Activity of Citrate Synthase (CS)

Tissue and Patient	cI	cII	cIII	cIV	cV	CS
Muscle:						
I.V.	10	25	ND	53	ND	210
S.S.	5	26	90	23	197	91
Normal	17–31	23–39	110–200	100–160	140–250	90–190
Fibroblasts:						
I.V.	4	17	58	17	35	109
S.S.	10	17	127	25	76	131
Normal	14–34	16–38	120–240	85–150	75–145	50–120

NOTE.—Data are calculated as nmol/min/mg protein. ND = not done; Normal = normal range.

Biochemical and Histochemical Assays

Specific activities of individual respiratory chain complexes were measured on cell and muscle homogenates.[16] Protein concentration was measured by the Folin-Ciocalteau method.[17] Specific activities of each complex were normalized to that of citrate synthase,[16] an indicator of the number of mitochondria.

Cytochrome c oxidase activity was visualized cytochemically in cell culture grown on a coverslip, washed twice in PBS containing 1 mg/ml $MgCl_2$ and 1 mg/ml $CaCl_2$, and air dried. Cells were preincubated for 15 min at room temperature in a buffer containing 50 mM Tris-HCl (pH 7.6), 1.2 mM $CoCl_2$, and 10% sucrose. They were rinsed once in 10% sucrose and 0.1-M Na phosphate (pH 7.6) and were incubated for 1–2 h at 37°C in 0.1-M Na phosphate buffer (pH 7.6), containing 2 mg/ml of cytochrome c, 1 mg/ml diaminobenzidine tetrahydrochloride, and 0.2 mg/ml catalase. Cells were rinsed once in 0.1-M Na phosphate buffer (pH 7.6) and 10% sucrose, once in PBS-Mg-$CaCl_2$, and once in distilled water. Coverslips were mounted in 50% glycerol-PBS and were visualized under a light microscope (NIKON Eclipse E400).

In Vivo Mitochondrial Translation Assay

Analysis of mitochondrial protein synthesis was performed following the protocol by Chomyn.[18] Cells at 70% confluence were labeled for 2 h with [^{35}S]-methionine-cysteine in the presence of 100 μg/ml emetine, an inhibitor of cytosolic protein synthesis. Samples were kept at −80°C until use. Equal amount of total cellular protein[17] were loaded on a 20% to 15% exponential gradient of polyacrylamide gel. The gel was then fixed and dried, and the mitochondrial translation products were visualized and measured densitometrically by a PhosphorImager apparatus (BioRad) by use of the Quantity One software provided by the manufacturer.

Homology Modeling

Each protein model was built using the automatic homology modeling server SWISS-MODEL.[19] The model of EFTu was built

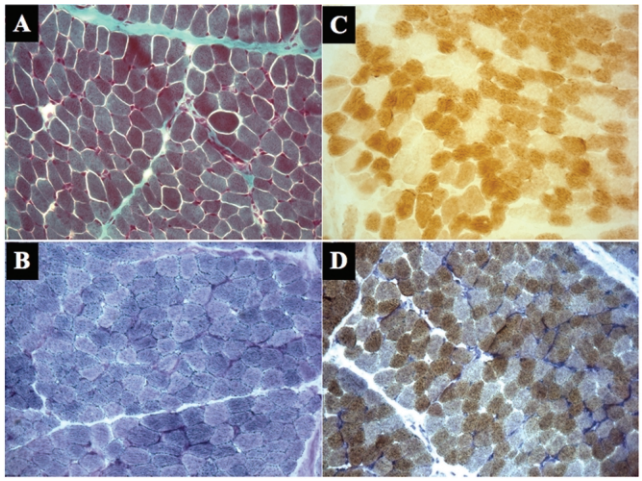

Figure 3. Light-microscopy examination of a muscle biopsy specimen from patient I.V. *A,* Modified Gomori trichrome staining. *B,* Succinate dehydrogenase (SDH) reaction. *C,* Cytochrome c oxidase (COX) reaction. *D,* SDH and COX reaction.

using the coordinates of the crystal structure of EFTu from *Bos taurus* (Protein Data Bank [PDB] 1D2E), which shows 96% sequence identity with the human homolog. Whatcheck[20] analysis confirmed the quality of the model.

The EFG model was built using the protein crystal structure from *Thermus thermophilus* (PDB 2BM0) that shares 40% of residues identical to the human sequence. Despite the relatively low sequence identity, this protein contains four highly conserved domains that make it a suitable homology-modeling target. In fact, the Whatcheck report shows that the overall model quality is only slightly lower in comparison to the EFTu model.

Structural analysis was made using VMD,[21] and secondary structure content was assigned by STRIDE.[22]

Yeast Strains, Media, and General Genetic Methods

Yeast strains are listed in table 2. Cells were cultured in YP (1% Bacto-yeast extract and 2% Bacto-peptone) or YNB medium (0.67% yeast nitrogen base without amino acids [Difco]), supplemented with the appropriate amino acids and bases for auxotrophy, at a final concentration of 40 μg/ml. Media were solidified with 20 g/liter agar. Glucose and ethanol were added at 2% (w/v), and glycerol at 3% (v/v). For the cytochrome absorption spectra, cells were grown to late-log phase in YNB medium supplemented with 0.5% glucose. Genetic procedures for crossing, sporulation, and tetrad dissection were performed by a standard protocol.[23] To obtain a heterozygous diploid *MEF1*/Δ*mef1* strain, a Δ*mef1 petite* mutant strain was crossed with the wild-type strain W303-1B.

Construction of Yeast Mutant Alleles

MEF1^{M516R} and *TUF1*^{R328Q} mutant alleles were produced by site-directed mutagenesis, by use of the QuikChange Kit (STRATAGENE). *MEF1* and *TUF1* wild-type genes cloned in pUC19 vector were used as template DNA. To obtain these plasmids, we PCR amplified DNA fragments of 3,018 bp (*MEF1*) and 2,596 bp (*TUF1*),[24] containing the ORFs and the 5′ and 3′ flanking regions (respectively, 629 bp and 653 for *TUF1* and 242 and 490 bp for *MEF1*), using genomic DNA of strain BY4741 as template and the appropriate forward and reverse primers containing restriction sites at their 5′ ends. To maximize the expression of the mutant allele, the preferred yeast codon encoding for either glutamine (CAA) or arginine (AGA) was used in the oligonucleotide sequences used for mutagenesis. Both wild-type and mutagenized inserts for each different construct were cloned in the pFL38 centromeric plasmid vector and sequence-verified on both strands. The sequences of the oligonucleotides used for cloning and sequencing *MEF1,* the base changes, and the corresponding modified primers used to generate mutated alleles are reported in table 3.

Southern-Blot Analysis in Yeast Strains

mtDNA was extracted by rapid mitochondrial preparation[25] from cells grown in YNB supplemented with 2% glucose. Aliquots of 1 μg of DNA were digested with *Eco*RV (Amersham). Southern-blot analysis was performed as described elsewhere.[26] Hybridization was performed by standard methods, with a 5′-[γ-^{32}P]ATP end-labeled yeast mtDNA-specific sequence repeat as a probe: 5′-CTCCTTTCGGGGTTCCGGCTCCCGTGGCCGGGCCCCGG-3′.

Miscellaneous Yeast Methods

Transformation of yeast strain was obtained by the lithium-acetate method.[27] Restriction-enzyme digestions, *Escherichia coli* transformation, and plasmid extractions were performed using standard methods.[28] Cytochrome spectra were determined as described elsewhere.[26]

Statistics

Two-tailed, unpaired Student's *t* test was used to calculate the significance of biochemical and molecular data. Statistical analysis was performed when four or more values were available for each category.

Results

Biochemical Assays and Mitochondrial Protein Synthesis

Multiple defects of mtDNA-dependent MRC complexes, particularly cI and cIV, were detected in the homogenates from muscle biopsies and skin-derived fibroblasts (table 4) taken at age 8 mo in both patients. The mtDNA-specific protein synthesis was severely reduced in fibroblasts from both patient I.V. and patient S.S., compared with control fibroblasts. Additional bands, which could not be attributed to a specific mtDNA protein species, were present in the high-molecular-weight range of both patients (fig. 2). The decrease varied for individual protein species—for instance, densitometric comparison between patients and controls gave a mean reduction of 87% for COX-I in both patients; of 74% and almost 95% for ND2 in patients I.V. and S.S., respectively; and of 70% and 88% for A6 in patients S.S. and I.V., respectively. ND1 was virtually undetectable in both patients.

Light-microscopy examination of the muscle biopsy specimen from patient I.V. showed diffusely increased fucsinophilia at the modified trichrome Gomori stain, with

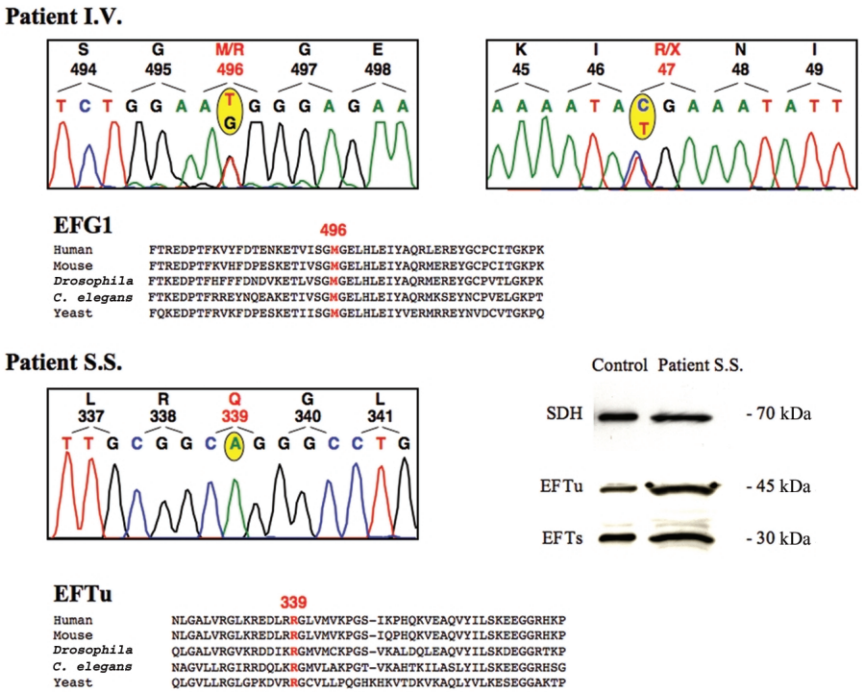

Figure 4. Molecular characterization of EFG1 and EFTu mutations. Below the sequencing profiles of EFG1 and EFTu genes in patients I.V. and S.S. are the ClustalW interspecies alignments of protein sequences from *H. sapiens* (Human), *Mus musculus* (Mouse), *Drosophila melanogaster, Caenorhabditis elegans,* and *S. cerevisiae* (Yeast). The mutant nucleotides are in yellow-shaded circles, and the mutant amino acid residues are labeled in red. Western blotting shows the presence of both EFTu and EFTs proteins in patient S.S. The 70-kDa succinate dehydrogenase (SDH) band was immunovisualized as a control.

mildly increased content of lipid and glycogen. Histochemically, the reaction specific to succinate dehydrogenase (part of cII), an MRC complex that does not contain mtDNA-encoded subunits, was increased, whereas the reaction specific to COX, which contains three mtDNA-encoded subunits, was reduced but not absent (fig. 3). Morphological analysis was not performed on the muscle biopsy sample from patient S.S.

Genetic Screening and Protein Western-Blot Analysis

Sequence analysis of the entire mtDNA from muscle of both patients failed to reveal mutations in either *syn* or *mit* genes, thus ruling out mtDNA as the disease-responsible genome. Since mitochondrial protein synthesis was severely impaired in both patients, we set up a candidate-gene strategy based on the screening of factors involved in mitochondrial translation. We first analyzed three genes in which mutations were already reported—namely, those encoding PUS1, EFG1, and MRPS16. In patient I.V., both *PUS1* and *MRPS16* sequences were normal, but we found two mutations in *EFG1,* a C→T transition at nucleotide position (np) 139 of the cDNA that causes the replacement of the amino acid residue R47 with a stop codon (TGA), and a T→G transversion at np 1478 that causes an M496R amino acid change (fig. 4). A heterozygous R47X was detected in the patient's father, whereas a heterozygous M496R was detected in the mother, thus proving that the mutations were allelic in the patient. The sister was heterozygous for the latter mutation.

No mutation in the above genes was found in patient S.S. Since her clinical presentation had features in common with that of I.V., including early onset, severe lactic acidosis, and predominant involvement of the CNS, we expanded the analysis to genes encoding two additional mitochondrial protein elongation factors—namely, EFTu and its auxiliary recycling factor, EFTs. No mutation was found in the *EFTs,* but a homozygous missense mutation was detected in *EFTu.* As shown in figure 4, this mutation, a G→A transition at np 1016 of the cDNA, converts the R residue at position 339 into a Q residue (R339Q). Both parents and the patient's brother were heterozygous for the mutation.

Western-blot analysis with the use of a specific antibody showed that the amount of EFTu protein detected in patient's skin fibroblasts was comparable to that in control fibroblasts (fig. 4). Neither mutation was found in DNA samples from 100 consecutive Italian control individuals.

Structural Modeling of Mutant EFG1^{M496R} and EFTu^{R339Q} Proteins

To make predictions about the structures of human EFG1 and EFTu and about the effects of the human EFG1^{M496R}

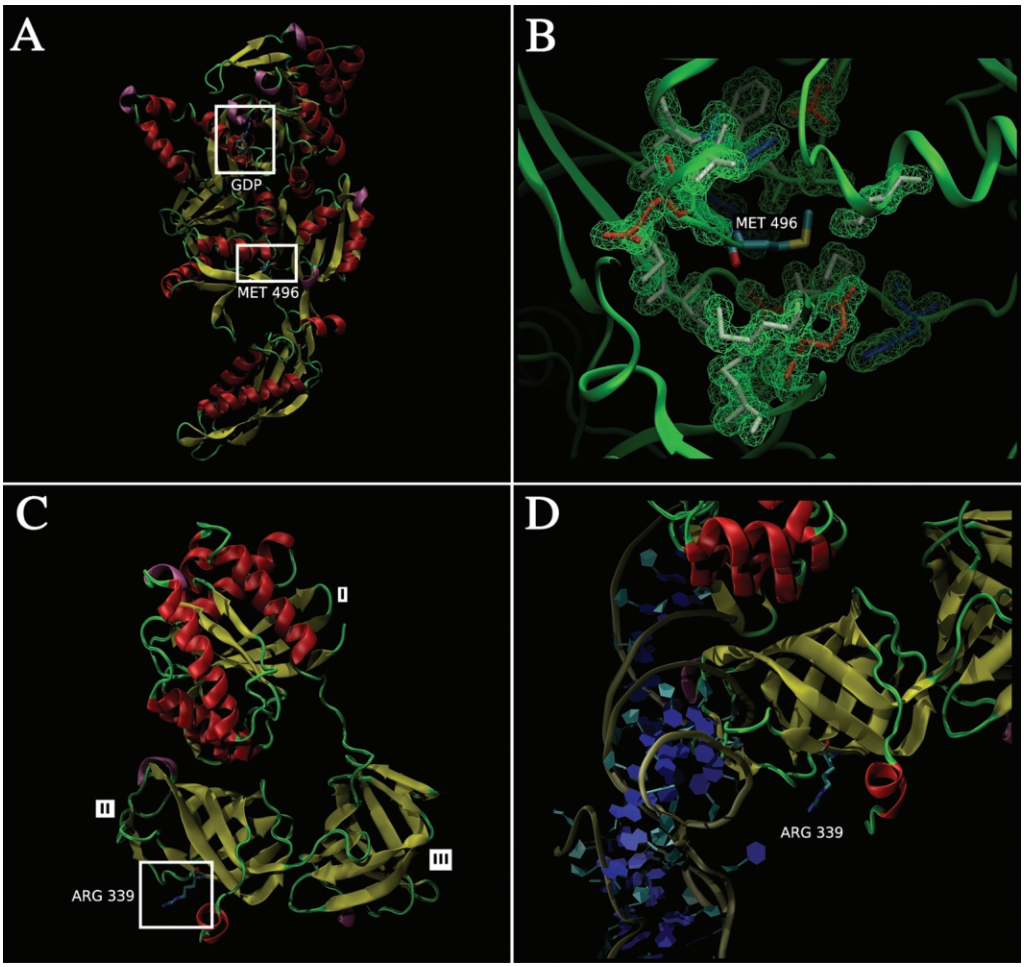

Figure 5. Modeling of mitochondrial EFG1 (*A* and *B*) and EFTu (*C* and *D*). In panel A, the EFG1 GDP-binding site and the wild-type M496 residue are indicated. In panel B, the pocket containing the M496 of EFG1 is magnified, and acidic, basic, and apolar residues are in red, blue, and gray, respectively. In panel C, the three domains and the Arg 339 residue of EFTu are labeled. In panel D, the model structure of human EFTu/tRNA complex is shown. The complex was obtained by superposing the bovine EFTu model on the crystal structure of the EFTu/tRNA complex of *T. aquaticus* (PDB 1TTT). The tRNA structure is in blue. The binding site for tRNA is magnified; note the position of the R339 residue, which is labeled for clarity.

and EFTu^{R339Q} missense mutations, we took advantage of information on the crystal structure of these proteins available for a mammalian organism, *B. taurus* (NCBI accession number NP_776632), and a micro-organism, *Thermus aquaticus* (NCBI accession number CAA46998).

Like other translocases, EFG1 is a single polypeptide with a molecular weight of ~80 kDa. As shown in figure 5*A*, the EFG1^{M496R} mutation is located at the end of an α-helix and before a β-sheet, in domain III of the mammalian protein.[29] Detailed analysis of this region, a pocket filled with both polar and apolar residues (fig. 5*B*), suggests that a direct effect of the M496R amino acid substitution on the EFG1 GTPase hydrolytic activity is unlikely, because the region is far from the GTP-binding site (fig. 5*A*). Rather, the replacement of the smaller, hydrophobic/negatively charged wild-type M with a bulkier, positively charged R residue is likely to produce a drastic structural rearrangement of the region that could, in turn, determine the destabilization of the entire protein or impede its correct interaction with the ribosome.

Human EFTu is also a GTPase consisting of a single polypeptide of ~45 kDa. The EFTu^{R339Q} mutation is located on a solvent-exposed β-sheet on the outer surface of domain II of mammalian EFTu[30] (fig. 5*C*). This position makes it unlikely that the R339Q mutation can determine a drastic structural rearrangement of the protein, because the interaction with neighboring amino acid residues is minimal. However, domain II constitutes the tRNA-binding site of EFTu[31] (fig. 5*D*); therefore, the most probable effect of the R339Q substitution is to hamper the formation of the

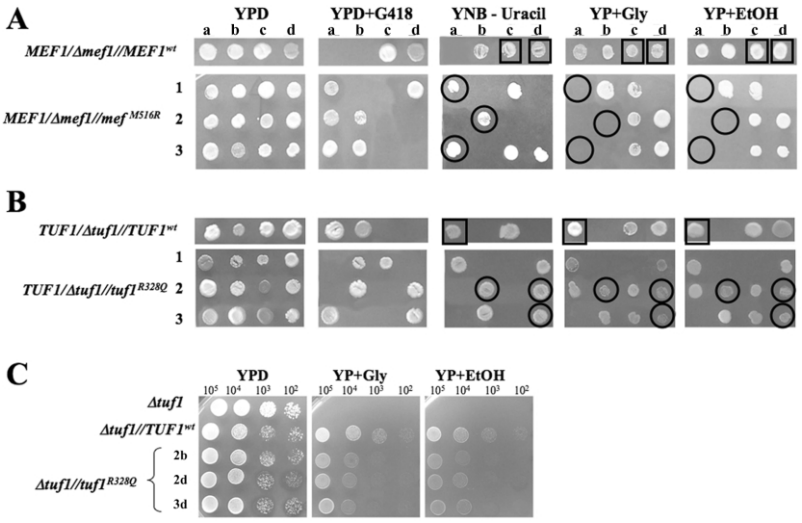

Figure 6. *A,* Tetrads analysis of *MEF1/Δmef1* diploid transformed with $MEF1^{wt}$ or $mef1^{M516R}$ alleles. The relevant genotype of the diploid strains is indicated on the left. One tetrad for the wild-type $MEF1/\Delta mef1//MEF1^{wt}$ transformant and three tetrads for the mutant $MEF1/\Delta mef1//mef1^{M516R}$ transformant are shown. Spore clones from the same tetrads are displayed horizontally (a–d). Since deletion of the *MEF1* gene was created by insertion of the *kanMX4* gene, which confers resistance to G418, the Δ*mef1* genotype is deduced by the ability to grow on yeast peptone dextrose medium (YPD) supplemented with G418. Since the genetic background is Δ*ura3* and the plasmid pFL38 used for all constructs carries the *URA3* wild-type allele, its presence is deduced by the ability to grow in the absence of uracil. A respiratory-proficient phenotype is deduced by the ability to grow on glycerol (Gly) and ethanol (EtOH). Black squares indicate the Δ*mef1* haploid strains transformed with the wild-type $MEF1^{wt}$ gene. Black circles indicate the Δ*mef1* haploid strains transformed with the $mef1^{M516R}$ mutant allele. *B,* Tetrads analysis of *TUF1/Δtuf1* diploid transformed with $TUF1^{wt}$ or $tuf1^{R328Q}$ alleles. The relevant genotype of the diploid strains is indicated on the left. The same experimental scheme described above for *MEF1* was applied to *TUF1*. Black squares indicate the Δ*tuf1* haploid strains transformed with the wild-type $TUF1^{wt}$ gene. Black circles indicate the Δ*tuf1* haploid strains transformed with the $tuf1^{R328Q}$ mutant allele. *C,* Oxidative growth phenotype in *TUF1* strains. Relevant genotype of the haploid Δ*tuf1* strains is indicated on the left. Rows 2b, 2d, and 3d refer to the corresponding spores reported in panel B. Equal amounts of serial dilutions of cells from exponentially grown cultures (10^5, 10^4, 10^3, and 10^2 cells) were spotted onto YP plates supplemented with 3% Gly or 2% EtOH. The growth was scored after 2 d of incubation at 28°C.

GTP:EFTu:aminoacyl-tRNA ternary complex. This hypothesis is supported by the demonstration that the amount and electrophoretic mobility of $EFTu^{R339Q}$ are both normal (fig. 4).

Complementation Studies in Yeast

To validate the pathogenic role of the missense mutations in mitochondrial EFG1 and EFTu in vivo, we set up ad hoc recombinant systems in the budding yeast *Saccharomyces cerevisiae,* a facultative aerobic organism. *MEF1* and *TUF1* are the yeast genes that encoded the orthologs of human mitochondrial EFG1 and EFTu. Mutant versions of these orthologs were expressed in *null* strains for each gene.

Inactivation of *MEF1* causes deletions in mtDNA that give rise to *petite* mutants.[32,33] Since the loss of a full-size mitochondrial genome is an irreversible process, mutant strains were obtained by sporulation and tetrad dissection of a heterozygous diploid *MEF1/Δmef1* strain transformed with either wild-type *MEF1* ($MEF1^{wt}$) or with mutant $mef1^{M516R}$ alleles. The $mef1^{M516R}$ mutation in yeast corresponds to the $EFG1^{M496R}$ mutation in humans. Diploid transformant clones will hereafter be indicated as $MEF1/\Delta mef1//MEF1^{wt}$ and $MEF1/\Delta mef1//mef1^{M516R}$. Likewise, a diploid *TUF1/Dtuf1* ρ^+ strain was transformed with either wild-type *TUF1* ($TUF1^{wt}$) or mutant $tuf1^{R328Q}$ alleles, with $tuf1^{R328Q}$ the yeast mutation corresponding to the $EFTu^{R339Q}$ human mutation. Diploid clones will be indicated as $TUF1/\Delta tuf1//TUF1^{wt}$ and $TUF1/\Delta tuf1//tuf1^{R328Q}$, respectively.

In the haploid transformant $\Delta mef1//mef1^{M516R}$, obtained from tetrad dissection, the mutant $mef1^{M516R}$ allele was completely unable to complement the oxidative growth defect of the Δ*mef1* strain (fig. 6*A*). In addition, the cytochrome spectrum profile of the Δ*mef1* and $\Delta mef1/mef1^{M516R}$ strains consistently lacked the peaks specific to cytochromes b and aa3, which are part of the mtDNA-dependent MRC complexes cIII and cIV, whereas the peak specific to cytochrome c, a nucleus-encoded protein, was normal (fig. 7*A*).

When the haploid transformant $\Delta mef1//mef1^{M516R}$ was grown on glucose-containing medium for three cycles, corresponding to ~25 generations, the percentage of respiratory-deficient (RD) mutant clones increased to virtually 100% (data not shown). The *petite* mutants can be

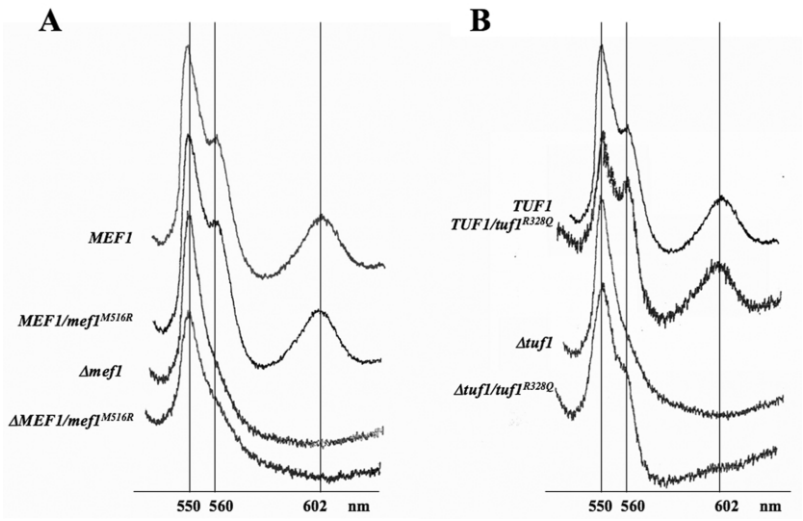

Figure 7. Reduced versus oxidized cytochrome spectra of *MEF1* (*A*) and *TUF1* (*B*) strains. The peak at 550 nm refers to cytochrome c, the peak at 560 nm refers to cytochrome b, and the peak at 602 nm refers to cytochrome aa3. The cytochrome amount is proportional to the height of the corresponding peak, relative to the baseline of each spectrum.

either ρ^- or ρ°. The ρ^- mutants contain deletion-carrying mtDNA, whereas ρ° mutants are mtDNA-less mutants. To evaluate the nature of the *petite* mutations (ρ^- vs. ρ°), we characterized mtDNA by Southern-blot analysis on RD clones carrying the *mef1*^{M516R} allele. Six of the eight clones were devoid of mtDNA, whereas two displayed rearranged mtDNA, indicating that the pathologic allele induced prevalently ρ° mutations (not shown).

Similar to *MEF1,* the inactivation of the *TUF1* gene causes deletions in mtDNA, giving rise to *petite* mutants.[32] In the transformant Δ*tuf1//tuf1*^{R328Q} strain, the *tuf1*^{R328Q} mutant allele partially complemented the oxidative growth defect of the Δ*tuf1* strain (fig. 6*B* and 6*C*). To evaluate whether the *tuf1*^{R328Q} mutation affected mtDNA stability, we measured the frequency of *petite* mutants in haploid Δ*tuf1* strains carrying either the *tuf1*^{R328Q} or the *TUF1*^{wt} allele. In the Δ*tuf1// tuf1*^{R328Q} strain, the petite frequency was indistinguishable from that of the Δ*tuf1// TUF1*strain (data not shown), indicating that the mutation did not affect mtDNA stability. The cytochrome spectrum profile of the Δ*tuf1* strain lacked both cytochrome b and aa3 peaks. The Δ*tuf1/tuf1*^{R328Q} strain showed the virtual absence of the peak corresponding to cytochrome aa3 but a less profound reduction of the peak corresponding to cytochrome b (fig. 7*B*). In both strains, the peak specific to cytochrome c was normal.

In *MEF1/*Δ*mef1//mef1*^{M516R} and *TUF1/*Δ*tuf1//tuf1*^{R328Q} heteroallelic diploid strains, oxidative growth and cytochrome profiles were similar to those of the wild-type haploid strains, indicating that both mutations behave as recessive traits in yeast, like the corresponding mutations do in humans.

Complementation Studies in Fibroblasts

To establish the specific role of the *EFG1*^{M496R} mutation in determining the OXPHOS-defective phenotype observed in mutant cells, we expressed recombinant wild-type *EFG1* (*EFG1*^{wt}) in an immortalized fibroblast cell line derived from patient I.V. Figure 8*A* shows the histochemical recovery of COX activity obtained in this cell line, compared with the profound COX defect of the parental culture. This result was confirmed by biochemical assay of MRC complexes cI and cIV in cell homogenate (fig. 8*B*). As shown in figure 8, we found a several-fold increase in the activities of transfected fibroblasts relative to the untransfected original cultures; this recovery reached ~80% for cI activity and ~40% for cIV activity, relative to the control mean. The histochemical and biochemical rescue was accompanied by recovery of mtDNA-specific translation (fig. 9). Similar results—consisting of histochemical COX recovery (fig. 8*A*); biochemical recovery of 79% for cI and 34% for cIV, relative to the control mean (fig. 8*B*); and clear recovery of mitochondrial protein translation (fig. 9)—were obtained by re-expressing wild-type EFTu (EFTu^{wt}) in immortalized fibroblasts from patient S.S. However, functional complementation occurred in EFTu^{R339Q} mutant cells transfected with EFTu^{wt} only when they were exposed for at least 1 d to a medium containing galactose instead of glucose as the major carbon source, whereas cells that were not treated with the galactose-containing medium failed to show any functional rescue, either in the activities of cI and cIV (fig. 8*A* and 8*B*) or in mitochondrial protein synthesis (fig. 9). The possibility that this result was because of a lack of expression of the EFTu^{wt} recombinant cDNA in transfected cells of patient S.S. was

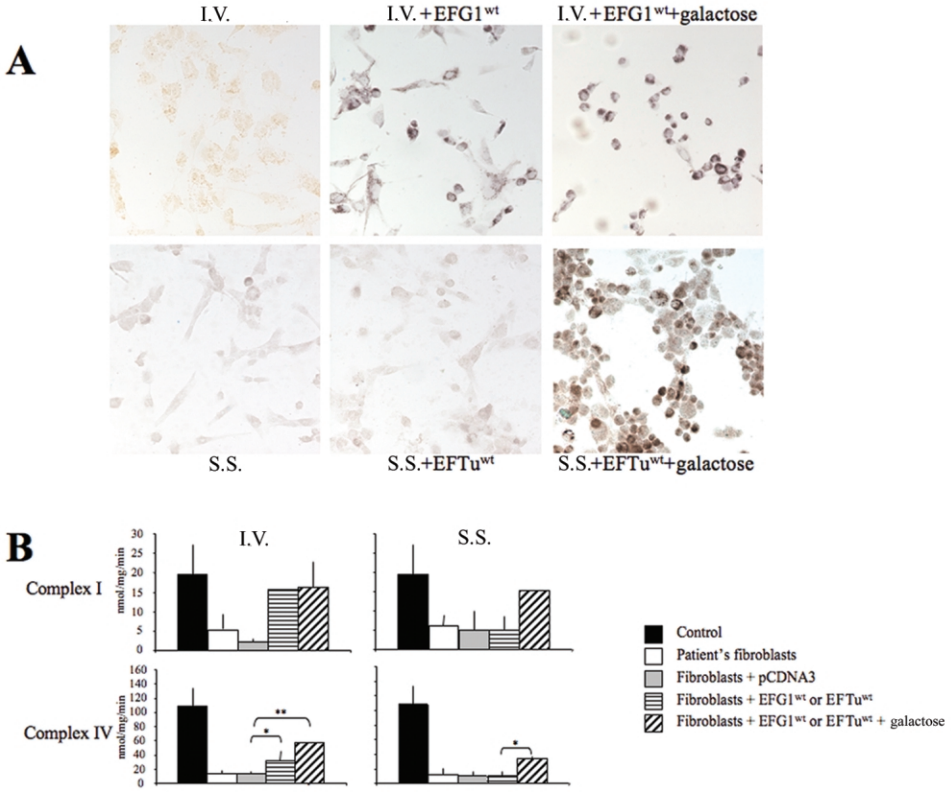

Figure 8. Complementation analysis in fibroblasts to determine histochemical and biochemical activities. *A,* COX-specific cytochemical reaction in immortalized fibroblasts cells from patients I.V. and S.S. and in the same cells after transfection with vectors expressing $EFG1^{wt}$ and $EFTu^{wt}$, grown in DMEM glucose medium, or after exposure for 1 d to DMEM galactose medium. *B,* Biochemical activities of cI and cIV in immortalized fibroblasts from patients I.V. and S.S. An asterisk (*) indicates Student's *t* test $P < .05$; a double asterisk (**) indicates $P < .01$. Statistical analysis was performed when four or more values were available for each category.

excluded by sequence analysis of retrotranscribed EFTu RNA, which showed the presence of both the wild-type and the mutant RNA species in an ~1:1 ratio (not shown). In contrast to glucose, galactose is a predominantly aerobic source of energy and is, in fact, used in selective medium to eliminate OXPHOS-incompetent mammalian cells. For instance, the OXPHOS-defective $EFTu^{R339Q}$ mutant cells, which either were not transfected or were transfected with an "empty" vector, all died after overnight exposure to the galactose selection medium (not shown).

Complementation Studies in Cell Hybrids and Cybrids

To further explore the unexpected behavior of $EFTu^{R339Q}$ mutant cells, we performed a series of experiments on hybrids generated by fusion of immortalized fibroblasts from our patients with a mtDNA-less 143B ρ° cell line. Selectable markers were exploited to obtain heterodikaryon cells—that is, hybrids derived from two cells of different parental origin (see the "Material and Methods" section)—which were confirmed by genotyping with suitable, highly polymorphic DNA markers (not shown). Fusions of *EFG1*^{M496R} defective cells with 143B ρ° cells showed the prompt recovery of robust histochemical (fig. 10*A*) and biochemical (fig. 10*B*) COX activity. However, when we repeated the same experiment, using the $EFTu^{R339Q}$ defective cell line, we observed neither histochemical nor biochemical recovery of COX activity (fig. 10*A* and 10*B*). Robust recovery of COX activity was documented in transmitochondrial cybrids derived from the fusion of 143B ρ° cells with cytoplasts from fibroblasts of patient S.S. (fig. 10*A* and 10*B*). Together with the data on mtDNA sequence analysis, this result further confirms that the biochemical and clinical phenotype of patient S.S. was not due to a primary defect of her mtDNA.

Discussion

Mitochondrial EFG1 is a five-domain GTPase, which catalyzes the translocation step of protein biosynthesis—that is, the movement of the peptidyl-tRNA-mRNA complex on the ribosome during protein elongation. This process consists in the transfer of the nascent peptidyl-tRNA from the ribosomal acceptor (amino acyl or A) site to the ribosomal peptidyl site and the consequent removal of an

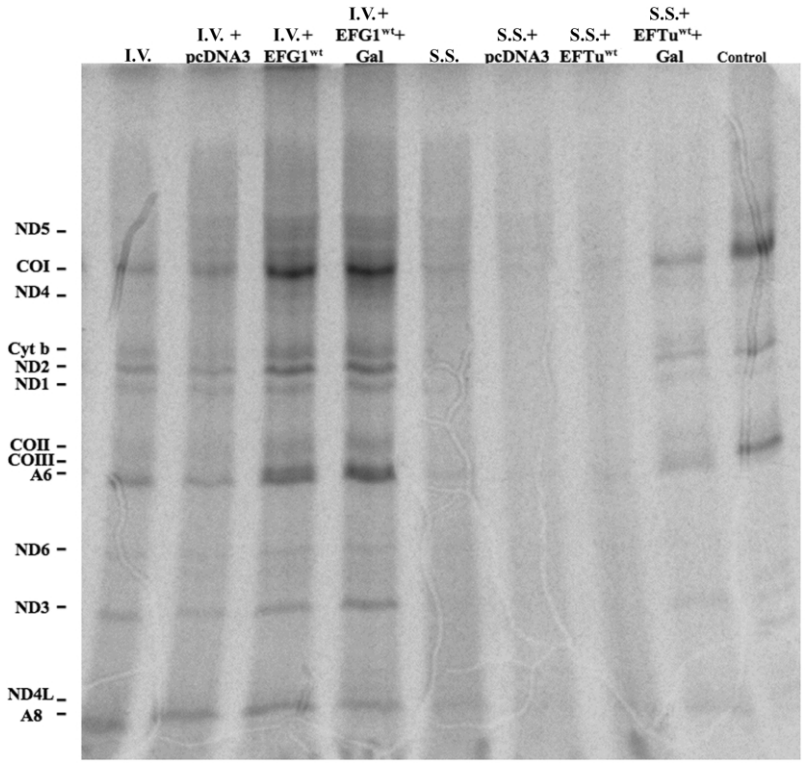

Figure 9. Complementation analysis in fibroblasts to determine mitochondrial protein synthesis. pCDNA3 indicates fibroblasts transfected with the pCDNA3 "empty" vector (no insert), EFG1^{wt} and EFTu^{wt} indicate fibroblasts transfected with vectors expressing the corresponding wild-type proteins, and Gal refers to fibroblasts exposed to galactose-containing medium. The bands are labeled as in figure 2.

uncharged tRNA from the peptidyl site to the ribosomal exit site.[34]

Patient I.V. was a compound heterozygote for two novel *EFG1* mutations: a stop mutation, which predicts the synthesis of a 46-aa polypeptide, and a missense mutation in a highly conserved amino acid residue of EFG1 domain III. The first reported EFG1-mutant patients were affected by severe neonatal liver failure.[7,8] In one patient, investigated by Antonicka et al.,[8] the EFG1 protein was undetectable in the liver, was very low in muscle and fibroblasts, but was only 60% lower than control levels in heart, thus paralleling the severity of the observed OXPHOS defect and organ failure. EFG1 expression in normal liver was found to be lower than in other tissues, again providing a possible explanation for the observed tissue specificity of the syndrome. No data are available concerning the expression of mitochondrial EFG1 in human brain, but the clinical features of our EFG1 mutant patient clearly indicate a primary involvement of the CNS, which overwhelmed, by far, that of other organs—notably, skeletal muscle, liver, and heart. Our patient never had laboratory or clinical signs of hepatic involvement. Her clinical course was dominated by severe, neonatal lactic acidosis and rapidly evolving neurological failure, with the neuroradiological hallmarks of early-onset Leigh syndrome—namely, bilateral necrotizing lesions in the basal ganglia, diencephalon, and brain stem.[35] A number of hypotheses can be formulated to explain these observations. For instance, specific mutations in different regions of the same EFG1 protein may have different effects on mitochondrial translation in different tissues, thereby dictating the specific clinical outcome of different individuals. It is also possible that adaptive mechanisms may act differently in different patients, thereby contributing to the observed clinical variability. This is the likely mechanism that could explain the recently reported association of the same mutation in mitochondrial EFTs with entirely distinct syndromes: an encephalomyopathy and a cardiomyopathy.[9] Another fact to be considered is that, in humans and other organisms, including yeast, there are two alleged isoforms of mitochondrial EFG—namely, EFG1 and EFG2—which raises the possibility that a defect of the former protein can be partly compensated by the activity of the latter, possibly in a tissue- and individual-specific fashion. This hypothesis is supported by the observation that human EFG2 is highly expressed in energy-consuming tissues, such as skeletal muscle, heart, and fetal liver, which contain a large number of mitochondria.[36] The functional role of EFG2, however, is uncertain; for instance, the ablation of yeast *MEF2,* the homolog of *EFG2,* is not associated

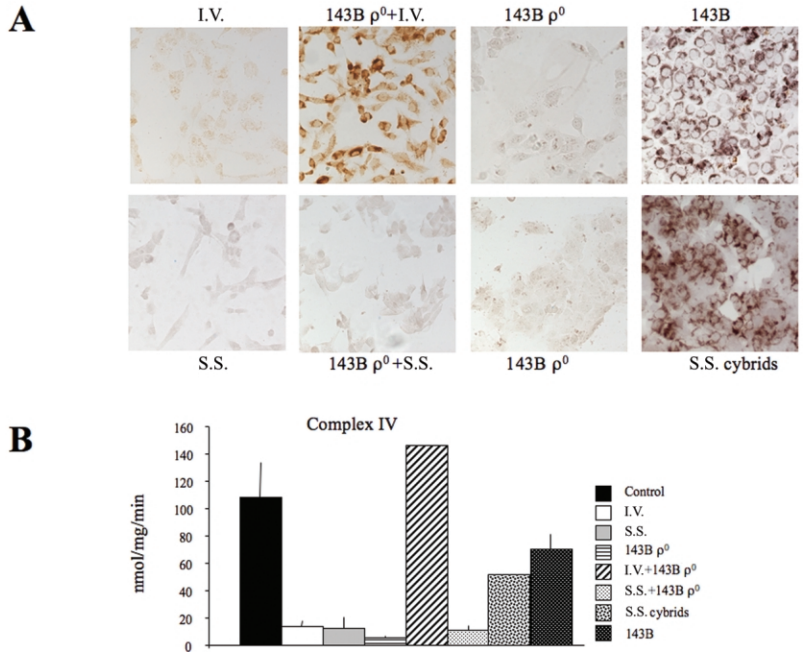

Figure 10. Complementation analysis in cell hybrids and cybrids. *A,* COX-specific cytochemical reaction in immortalized fibroblast cells from patients I.V. and S.S., 143B ρ^0 cells, 143B progenitor cells, transmitochondrial cybrids, and heterodikaryon hybrids. *B,* Biochemical activities of cIV in fibroblasts, 143B ρ^0 cells, 143B progenitor cells, transmitochondrial cybrids, and heterodikaryon hybrids.

with an OXPHOS phenotype, as is the case for *MEF1,* the homolog of EFG1, the ablation of which causes an extremely drastic *petite* ρ^0 phenotype.

Our second patient, S.S., carried the first mutation ever reported in mitochondrial EFTu (R339Q). Like EFG1, EFTu is a GTPase. The GTP:EFTu activated complex loads an aminoacyl-tRNA from its specific transferase, escorts it to the ribosomal A site, and is then released from the ribosome as an EFTu:GDP inactive complex. This complex is the substrate of EFTs, which promotes the exchange of GDP with GTP on EFTu, thus reactivating it. Patient S.S. had an extremely severe syndrome, dominated by lactic acidosis and rapidly fatal encephalopathy, with diffuse cystic leukodystrophy and micropolygyria, a developmental abnormality of the brain that occurs well before birth. Modest elevation of hepatic enzymes in blood and episodic hyperammonemia indicated mild liver involvement that never progressed into hepatic failure. Other tissues, notably the heart, were clinically spared. The identification of other patients with mutations will show to what extent the brain abnormalities of our patient S.S. are specific to EFTu mutation.

The deleterious effects of the mutations on mitochondrial EFG1 and EFTu were predicted by modeling studies on their crystal structures, and their consequences for OXPHOS were validated by functional studies in both yeast and mammalian recombinant systems. The missense mutations found in our patients hit amino acid residues that are conserved from mammals to the facultative aerobic yeast *S. cerevisiae* (fig. 4).

The *MEF1*-defective yeast strain (Δ*mef1*) displays an OXPHOS phenotype characterized by failure to grow in media containing glycerol, ethanol, or other obligatory aerobic compounds as the only carbon sources. No correction was obtained by re-expressing, in the Δ*mef1* strain, a *mef1* variant harboring $mef1^{M516R}$, a mutation equivalent to human $EFG1^{M496R}$. The OXPHOS phenotype of the Δ*mef1* strain is associated with mtDNA instability, which, in turn, determines increased segregation of RD *petite* mutants.[37] When the Δ*mef1* strain re-expressing the $mef1^{M516R}$ mutant allele was grown in a glucose-containing medium, it produced virtually 100% RD mutant clones, indicating, for this mutation, a nearly complete loss of function. Taken together, these results indicate that the *EFG1* mutation found in humans is deleterious in yeast.

The yeast $tuf1^{R328Q}$, equivalent to human $EFTu^{R339Q}$, gave a clearly defective OXPHOS phenotype, less drastic, however, than that of the Δ*TUF1 null* strain, indicating the preservation of some functional competency. In particular, aerobic growth was reduced but not abolished in the Δ*tuf1*// $tuf1^{R328Q}$ strain, and, although the decrease of cytochrome aa3, which is part of COX, was marked, that of cytochrome b, which is part of cIII, was much milder than in the Δ*mef1* strain. It is interesting that the effects on cytochrome content of the $tuf1^{R328Q}$ mutation are similar to those produced by chloramphenicol, an inhibitor of mitochondrial protein synthesis.[38] The "leaky" phenotype observed in yeast is in contrast to the extremely severe biochemical and translational defects found in $EFTu^{R339Q}$ human mitochondria. A possible explanation for this dis-

crepancy is that the orthology of yeast tuf1 to mammalian EFTu is imperfect, because the former combines, in a single polypeptide, the functions of both EFTu and EFTs.

In complementation experiments performed on mammalian cell cultures, we observed that the multiple defects of MRC activities and the profound decrease of mtDNA translation were both corrected by re-expression of either $EFG1^{wt}$ or $EFTu^{wt}$ in the corresponding mutant fibroblast cell lines. These results confirm the pathogenic role of the $EFG1^{M496R}$ and $EFTu^{R339Q}$ mutant alleles in causing OXPHOS failure and disease. However, in contrast to the $EFG1^{wt}$-transfected $EFG1^{M496R}$ mutant cells, the phenotype rescue of the $EFTu^{wt}$-transfected $EFTu^{R339Q}$ mutant cells was obtained only by use of a strictly aerobic growth medium, which selects cells for OXPHOS competency. This result was confirmed by the persistence of faulty COX activity in heterodikaryon hybrids obtained by fusion of $EFTu^{R339Q}$ mutant cells and 143B ρ° cells, whereas the hybrids between $EFG1^{M496R}$ and 143B ρ° cells had nearly normal COX activity.

The refractoriness of $EFTu^{R339Q}$ mutant cells to functional complementation remains unexplained. One possibility is the coexistence of a *syn* mutation in mtDNA, but it was excluded by sequencing of the entire mtDNA of patient S.S. However, several other hypotheses can be formulated to explain this unexpected behavior. For instance, the $EFTu^{R339Q}$ could exert a dominant negative effect in cell culture, which is compatible with the persistence of the mutant protein in fibroblasts (fig. 4) but is baffling for a genetic defect that is clearly recessive in carriers and affected individuals. A second possibility is that the OXPHOS rescue could be limited by the relative amount of EFTs compared with EFTu, as suggested by the leaky phenotype of the $\Delta tuf1//tuf1^{R328Q}$ mutant yeast strain. A third possibility is that $EFTu^{wt}$ itself could inhibit translation when overexpressed, as recently proposed for both EFTu[8] and EFTs.[9]

Future work is warranted to challenge these hypotheses—for instance, by titration of the expression of recombinant $EFTu^{R339Q}$ or $EFTu^{wt}$ in normal cells and by coexpression of recombinant $EFTu^{wt}$ and $EFTs^{wt}$ in $EFTu^{R339Q}$ mutant cells.

The two patients described here were part of a cohort of six infantile cases with a common biochemical signature: multiple MRC defects in muscle and cultured fibroblasts. Of the four remaining patients, two brothers affected by MLASA had a homozygous mutation in PUS1,[39] whereas the other two involve cases that are still undefined at the molecular level. Although limited in number, these observations and similar findings recently reported by others[4,6–9] contribute to define a new, rapidly expanding group of nuclear gene defects that could account for a substantial fraction of mitochondrial disorders of infancy and childhood. In addition, these results reveal the existence of complex, and partly unexpected, checkpoint mechanisms regulating mtDNA protein synthesis. The elucidation of these mechanisms can help us understand the biology of mtDNA homeostasis and the pathophysiology of its defects.

Acknowledgments

We are indebted to Barbara Geehan for revising the manuscript. We are grateful to Prof. Linda Spremulli for the generous gift of an anti-EFTu and -EFTs antibody, to Prof. Rodney Rothstein for the generous gift of the W303-1B yeast strain, to Dr. Alessandro Prelle for skillful histoenzymatic analysis of skeletal muscle, and to Dr. Marianna Bugiani for critical discussion of MRI data. This study was supported by Fondazione Telethon-Italy (grant GGP030039), Fondazione Pierfranco e Luisa Mariani, MITOCIRCLE, and EUMITOCOMBAT (LSHM-CT-2004-503116) network grants from the European Union Framework Program 6.

Web Resources

Accession numbers and URLs for data presented herein are as follows:

ClustalW, http://www.ebi.ac.uk/clustalw/
Euroscarf, http://web.uni-frankfurt.de/fb15/mikro/euroscarf/
Mitomap, http://www.mitomap.org/
NCBI, http://www.ncbi.nlm.nih.gov/ (for EFG1 *H. sapiens* [accession number Q96RP9], *M. musculus* [accession number Q8K0D5], *D. melanogaster* [accession number Q9VM33], *C. elegans* [accession number Q9XV52], and *S. cerevisiae* [accession number P25039] and EFTu *H. sapiens* [accession number P49411], *M. musculus* [accession number Q8BFR5], *B. taurus* [accession number NP_776632], *D. melanogaster* [accession number Q86NS6], *C. elegans* [accession number P02992], *S. cerevisiae* [accession number Q19072], and *T. aquaticus* [accession number CAA46998])
Online Mendelian Inheritance in Man (OMIM), http://www.ncbi.nlm.nih.gov/Omim/ (for MLASA, MRPS16, and combined oxidative phosphorylation deficiency 1)
PDB, http://www.rcsb.org/pdb
RZPD German Resource Center, http://www.rzpd.de/

References

1. Schapira AH (2006) Mitochondrial disease. Lancet 368:70–82
2. Jacobs HT, Turnbull DM (2005) Nuclear genes and mitochondrial translation: a new class of genetic disease. Trends Genet 21:312–314
3. Sylvester JE, Fischel-Ghodsian N, Mougey EB, O'Brien TW (2004) Mitochondrial ribosomal proteins: candidate genes for mitochondrial disease. Genet Med 6:73–80
4. Bykhovskaya Y, Casas K, Mengesha E, Inbal A, Fischel-Ghodsian N (2004) Missense mutation in pseudouridine synthase 1 (PUS1) causes mitochondrial myopathy and sideroblastic anemia (MLASA). Am J Hum Genet 74:1303–1308
5. Patton JR, Bykhovskaya Y, Mengesha E, Bertolotto C, Fischel-Ghodsian N (2005) Mitochondrial myopathy and sideroblastic anemia (MLASA): missense mutation in the pseudouridine synthase 1 (PUS1) gene is associated with the loss of tRNA pseudouridylation. J Biol Chem 280:19823–19828
6. Miller C, Saada A, Shaul N, Shabtai N, Ben-Shalom E, Shaag A, Hershkovitz E, Elpeleg O (2004) Defective mitochondrial translation caused by a ribosomal protein (MRPS16) mutation. Ann Neurol 56:734–738
7. Coenen MJ, Antonicka H, Ugalde C, Sasarman F, Rossi R,

Heister JG, Newbold RF, Trijbels FJ, van den Heuvel LP, Shoubridge EA, et al (2004) Mutant mitochondrial elongation factor G1 and combined oxidative phosphorylation deficiency. N Engl J Med 351:2080–2086
8. Antonicka H, Sasarman F, Kennaway NG, Shoubridge EA (2006) The molecular basis for tissue specificity of the oxidative phosphorylation deficiencies in patients with mutations in the mitochondrial translation factor EFG1. Hum Mol Genet 15:1835–1846
9. Smeitink JAM, Elpeleg O, Antonicka H, Diepstra H, Saada A, Smits P, Sasarman F, Vriend G, Jacob-Hirsch J, Shaag A, et al (2006) Distinct clinical phenotype associated with a mutation in the mitochondrial translation factor EFTs. Am J Hum Genet 79:869–877
10. Tiranti V, Savoia A, Forti F, D'Apolito MF, Centra M, Rocchi M, Zeviani M (1997) Identification of the gene encoding the human mitochondrial RNA polymerase (h-mtRPOL) by cyberscreening of the Expressed Sequence Tags database. Hum Mol Genet 6:615–625
11. Munaro M, Tiranti V, Sandona D, Lamantea E, Uziel G, Bisson R, Zeviani M (1997) A single cell complementation class is common to several cases of cytochrome c oxidase-defective Leigh's syndrome. Hum Mol Genet 6:221–228
12. Tiranti V, Munaro M, Sandona D, Lamantea E, Rimoldi M, DiDonato S, Bisson R, Zeviani M (1995) Nuclear DNA origin of cytochrome c oxidase deficiency in Leigh's syndrome: genetic evidence based on patient's-derived rho degrees transformants. Hum Mol Genet 4:2017–2023
13. Fernandez-Vizarra E, Lopez-Perez MJ, Enriquez JA (2002) Isolation of biogenetically competent mitochondria from mammalian tissues and cultured cells. Methods 26:292–297
14. Tiranti V, Galimberti C, Nijtmans L, Bovolenta S, Perini MP, Zeviani M (1999) Characterization of SURF-1 expression and Surf-1p function in normal and disease conditions. Hum Mol Genet 8:2533–2540
15. Woriax VL, Bullard JM, Ma L, Yokogawa T, Spremulli LL (1997) Mechanistic studies of the translational elongation cycle in mammalian mitochondria. Biochim Biophys Acta 1352:91–101
16. Bugiani M, Invernizzi F, Alberio S, Briem E, Lamantea E, Carrara F, Moroni I, Farina L, Spada M, Donati MA, et al (2004) Clinical and molecular findings in children with complex I deficiency. Biochim Biophys Acta 1659:136–147
17. Lowry OH, Rosebrough NJ, Farr AL, Randall RJ (1951) Protein measurement with the Folin phenol reagent. J Biol Chem 193:265–275
18. Chomyn A (1996) *In vivo* labeling and analysis of human mitochondrial translation product. Methods Enzymol 264: 197–211
19. Schwede T, Kopp J, Guex N, Peitsch MC (2003) SWISS-MODEL: an automated protein homology-modeling server. Nucleic Acids Res 31:3381–3385
20. Hooft RW, Vriend G, Sander C, Abola EE (1996) Errors in protein structures. Nature 381:272
21. Humphrey W, Dalke A, Schulten K (1996) VMD—visual molecular dynamics. J Mol Graph 14:33–38
22. Frishman D, Argos P (1995) Knowledge-based protein secondary structure assignment. Proteins 23:566–579
23. Sherman F, Fink GR, Hicks JB (1986) Laboratory course manual for methods in yeast genetics. Cold Spring Harbor Laboratory, New York
24. Nagata S, Tsunetsugu-Yokota Y, Naito A, Kaziro Y (1983) Molecular cloning and sequence determination of the nuclear gene coding for mitochondrial elongation factor Tu of *Saccharomyces cerevisiae*. Proc Natl Acad Sci USA 80:6192–6196
25. Defontaine A, Lecocq FM, Hallet JN (1991) A rapid miniprep method for the preparation of yeast mitochondrial DNA. Nucleic Acids Res 19:185
26. Fontanesi F, Palmieri L, Scarcia P, Lodi T, Donnini C, Limongelli A, Tiranti V, Zeviani M, Ferrero I, Viola AM (2004) Mutations in AAC2, equivalent to human adPEO-associated ANT1 mutations, lead to defective oxidative phosphorylation in *Saccharomyces cerevisiae* and affect mitochondrial DNA stability. Hum Mol Genet 13:923–934
27. Gietz RD, Woods RA (2002) Transformation of yeast by the LiAc/SS carrier DNA/PEG method. Methods Enzymol 350:87–96
28. Sambrook J, Russel DW (2001) Molecular cloning: a laboratory manual. Cold Spring Harbor Laboratory Press, Cold Spring Harbor, NY
29. Czworkowski J, Wang J, Steitz TA, Moore PB (1994) The crystal structure of elongation factor G complexed with GDP, at 2.7 resolution. EMBO J 13:3661–3668
30. Jeppesen MG, Navratil T, Spremulli LL, Nyborg J (2005) Crystal structure of the bovine mitochondrial elongation factor Tu·Ts complex. J Biol Chem 280:5071–5081
31. Hunter SE, Spremulli LL (2004) Interaction of mitochondrial elongation factor Tu with aminoacyl-tRNAs. Mitochondrion 4:21–29
32. Vambutas A, Ackerman SH, Tzagoloff A (1991) Mitochondrial translational-initiation and elongation factors in *Saccharomyces cerevisiae*. Eur J Biochem 201:643–652
33. Myers AM, Pape LK, Tzagoloff A (1985) Mitochondrial protein synthesis is required for maintenance of intact mitochondrial genomes in *Saccharomyces cerevisiae*. EMBO J 4:2087–2092
34. Wintermeyer W, Peske F, Beringer M, Gromadski KB, Savelsbergh A, Rodnina MV (2004) Mechanisms of elongation on the ribosome: dynamics of a macromolecular machine. Biochem Soc Trans 32:733–737
35. Farina L, Chiapparini L, Uziel G, Bugiani M, Zeviani M, Savoiardo M (2002) MR findings in Leigh syndrome with COX deficiency and SURF-1 mutations. AJNR Am J Neuroradiol 7: 1095–1100
36. Hammarsund M, Wilson W, Corcoran M, Merup M, Einhorn S, Grander D, Sangfelt O (2001) Identification and characterization of two novel human mitochondrial elongation factor genes, hEFG2 and hEFG1, phylogenetically conserved through evolution. Hum Genet 109:542–550
37. Mounolou JC, Jakob H, Slonimski PP (1966) Mitochondrial DNA from yeast "petite" mutants: specific changes in buoyant density corresponding to different cytoplasmic mutations. Biochem Biophys Res Commun 24:218–224
38. Cottrell SF, Rabinowitz M, Getz GS (1975) Cytochrome synthesis in synchronous cultures of the yeast *Saccharomyces cerevisiae*. J Biol Chem 250:4087–4094
39. Fernandez-Vizarra, Berardinelli A, Valente L, Tiranti V, Zeviani M (2006) Nonsense mutation in pseudouridylate synthase 1 (PUS1) in two brothers affected by myopathy, lactic acidosis and sideroblastic anemia (MLASA). J Med Genet (http://jmg.bmj.com/cgi/rapidpdf/jmg.2006.045252v1) (electronically published October 20, 2006; accessed November 14, 2006)